Available online at www.sciencedirect.com
ScienceDirect
Bioorganic & Medicinal Chemistry 15 (2007) 5003–5017
Bioorganic & Medicinal Chemistry

N9-Benzyl-substituted 1,3-dimethyl- and 1,3-dipropyl-pyrimido[2,1-*f*]purinediones: Synthesis and structure–activity relationships at adenosine A_1 and A_{2A} receptors

Anna Drabczyńska,[a] Christa E. Müller,[b] Janina Karolak-Wojciechowska,[c] Britta Schumacher,[b] Anke Schiedel,[b] Olga Yuzlenko[a] and Katarzyna Kieć-Kononowicz[a,*]

[a]*Jagiellonian University, Medical College, Faculty of Pharmacy, Department of Technology and Biotechnology of Drugs, Medyczna 9, Pl 30-688 Kraków, Poland*
[b]*Pharmaceutical Institute, University of Bonn, An der Immenburg 4, D-53121 Bonn, Germany*
[c]*Institute of General and Ecological Chemistry, Technical University of Łódź, Żwirki 36, Pl 90-924 Łódź, Poland*

Received 14 July 2006; revised 30 March 2007; accepted 13 April 2007
Available online 19 April 2007

Abstract—Synthesis and physicochemical properties of *N*-benzyl pyrimido[2,1-*f*]purinediones are described. These derivatives were synthesized by the cyclization of 7-chloropropylo-8-bromo-1,3-dimethyl- or 1,3-dipropyl xanthine derivatives with corresponding (un)substituted benzylamines. Dipropyl derivatives were obtained under microwave irradiation conditions either. The obtained compounds (**1**–**20**) were evaluated for their affinity to adenosine A_1 and A_{2A} receptors, selected compounds were additionally investigated for affinity to the A_3 receptor subtype. The results of the radioligand binding assays to A_1 and A_{2A} adenosine receptors showed that most of the 1,3-dimethyl-9-benzylpyrimidopurinediones exhibited selective affinity to A_{2A} receptors at micromolar or submicromolar concentrations (for example, derivative **9** with *o*-methoxy substituent displayed a K_i value of 0.699 μM at rat A_{2A} receptor with more than 36-fold selectivity). Contrary to previously described arylpyrimido[2,1-*f*]purinediones dipropyl derivatives (compounds **15**–**20**) showed affinity to both kinds of receptors increased, however A_1 affinity increased to a larger extent, with the result that A_{2A} selectivity was abolished. The best adenosine A_1 receptor ligand was *m*-chlorobenzyl derivative **18** (K_i = 0.089 μM and 5-fold A_1 selectivity). Structure–activity relationships were discussed with the analysis of lipophilic and spatial properties of the investigated compounds. Pharmacophore model of adenosine A_1 receptor antagonist was adopted for this purpose.

1. Introduction

The physiological effects of extracellular adenosine are mediated by four G-protein coupled receptors: A_1, A_{2A}, A_{2B} and A_3 adenosine receptors (ARs).[1,2] The ARs may either inhibit (A_1, A_3) or stimulate (A_{2A}, A_{2B}) adenylate cyclase activity. Coupling to other second messenger systems has been described, including phospholipase C stimulation (A_1, A_{2B}, A_3).[3] Selective A_1 AR antagonists have demonstrated promising therapeutic potential for the treatment of cognitive diseases, renal failure, Alzheimer's disease and cardiac failure.[4] In the central nervous system the A_{2A} ARs are present in high density in basal ganglia and are able to cross-talk with dopamine receptors.[5,6] Adenosine A_{2A} receptor antagonists may be useful for the treatment of acute and chronic neurodegenerative disorders such as cerebral ischemia, Parkinson's and Huntington's diseases, as drugs controlling motor functions and exhibiting neuroprotective properties.[7–11]

The involvement of AR interaction in seizure disorders has been discussed.[7,10–14] Adenosine and specific AR agonists exert potent anticonvulsant effects in a variety of seizure models, primarily via activation of the A_1 AR subtype. AR antagonists were described to produce proconvulsant effects.[10,12–14]

Since ARs offer an attractive target for drug development several studies were carried out in order to find subtype-selective AR antagonists.[15–22] Styryl xanthines have been recognized as potent and selective adenosine A_{2A} receptor antagonists (Fig. 1). The first very potent

Keywords: Adenosine A_1; A_{2A} receptor antagonists; Pyrimido[2,1-*f*]purinediones; Tricyclic xanthine derivatives.
* Corresponding author. Tel./fax: +48 12 657 04 88; e-mail: mfkonono@cyf-kr.edu.pl

0968-0896/$ - see front matter © 2007 Elsevier Ltd. All rights reserved.
doi:10.1016/j.bmc.2007.04.018

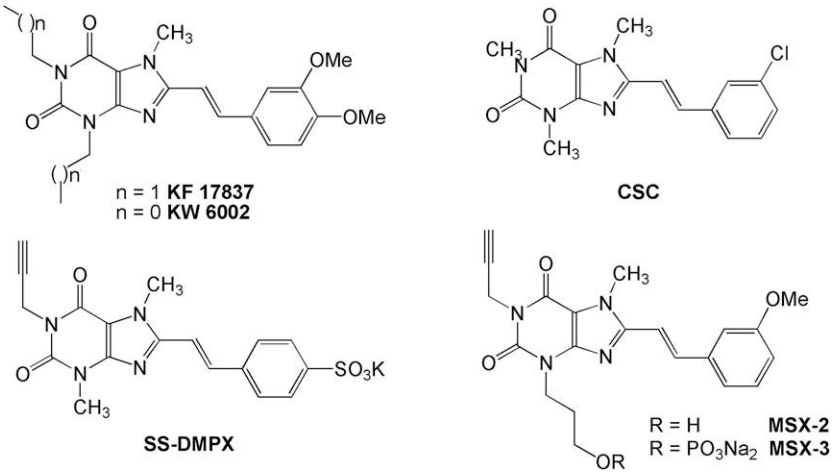

Figure 1. Structures of styryl xanthines with adenosine A_{2A} receptor antagonistic properties.

and selective A_{2A} adenosine receptor antagonists were KF 17837[23,24] and CSC.[25] KF 17837, being more potent A_{2A} adenosine receptor antagonist than CSC, was less selective vs A_1 adenosine receptor subtype. Two major problems are connected with this group of compounds: low water solubility[26] and rapid photoisomerisation.[27,28] To enhance water solubility of styryl xanthines two main approaches have been used by Müller and coworkers: introduction of polar groups on the phenyl ring (SS-DMPX)[29] or preparation of phosphate pro-drugs (MSX-2, MSX-3).[30] Compound KW-6002 is being evaluated in phase II clinical trials as potential antiparkinsonian and antidepressant drug.[31,32]

In our studies we focused on the search for A_1/A_{2A} AR ligands among tricyclic xanthine derivatives.[16,33–35] Compounds (**I**) with oxygen or nitrogen containing fused rings were obtained[16,33,34] as constrained analogues of 8-styrylxanthines (Fig. 2).[18,36] Thus imidazo-, pyrimido- and 1,3-diazepino[2,1-*f*]purinediones were synthesized (**I**). One series of compounds (**II**) possessed variously substituted aryl moiety placed directly at the nitrogen atom of the fused ring. In vitro studies have shown their A_{2A} AR affinity and selectivity, in vivo some of the compounds displayed anticonvulsant activity. The pyrimidine annelated ring (**II**) was beneficial for both receptor affinity and anticonvulsant activity. Continuing our research in the group of tricyclic derivatives of purinediones[16,33,34] pyrimido[2,1-*f*]purinediones with (un)substituted benzyl moieties at the annelated ring were synthesized. Such compounds (**III**), possessing aryl substituent placed in the greater (two bonds) distance from the nitrogen atom of the annelated ring, were designed as better mimicking the structure of styryl xanthines.

To gain insight into the structure affinity relationships of this class of compounds, the lead structure benzylpyrimidotheophylline (**1**) was modified by:

- elongation of R^1 substituents (replacement of the methyl groups in theophylline by propyl groups as in the standard xanthine A_1 antagonist 8-cyclopentyl-1,3-dipropylxanthine (DPCPX)),
- introducing R^2 substituent to the benzyl methylene,
- introducing R^3 substituent in position *o*-, *m*- or *p*- of the aromatic ring,

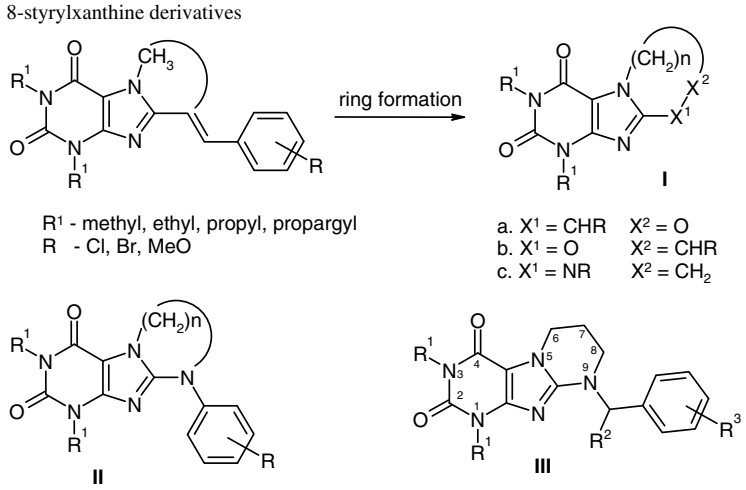

Figure 2. Oxygen or nitrogen containing annelated xanthine derivatives as constrained analogues of 8-styryl xanthines.

- replacement of the phenyl ring by the potentially bioisosteric heterocycles furane or pyridine.

The synthesized compounds were evaluated in vitro for their affinity to ARs. Physicochemical properties of tested compounds were estimated by means of calculations. In order to analyze three-dimensional properties of this group of compounds structure examination was performed by means of molecular modelling and X-ray analysis for two selected compounds.

2. Chemistry

The synthesis of tricyclic 1,3-dimethylpyrimidopurinedione with benzyl substituents in the 9-position of the annelated ring was accomplished as shown in Figure 3. As starting material 7-(3-chloropropyl)-8-bromotheophylline was used which was obtained as previously described.[37] The compound was reacted with the substituted in *o*-, *m*- or *p*-position benzylamines under various reaction conditions with regard to the amount of amine, solvent, and reaction time. The data are summarized in Table 1.

The synthesis of compounds **1** and **12** had been described previously,[38] but their structures had only been determined by UV spectra and no biological activity has been reported.

For the preparation of 1,3-dipropylxanthine as starting material for cyclization to the corresponding dipropyl-substituted pyrimidopurinediones standard procedures were applied.[39,40] Subsequent bromination, introduction of the chloropropyl chain in position 7 by two phase alkylation with 1-chloro-3-bromopropane followed by cyclization with benzylamines yielded the target tricyclic 9-benzyl-substituted compounds (Fig. 3).

Alternatively, dipropyl derivatives **15**–**20** could also be prepared by microwave flash-heating method. Thus, 8-bromo-7-(3-chloropropyl)-1,3-dipropylxanthine was melted with the appropriate benzylamine in a microwave oven (power 300–750 W) for 4–7 min.

Although the yields of the traditional and microwave method were comparable, the advantages of the last one were a dramatically reduced reaction time and a better quality (higher purity) of the products.

The structures of the synthesized compounds were confirmed by UV, IR and ^{1}H NMR spectra. The UV spectra showed a bathochromic shift of λ_{max} from ca. 276 nm to about 300 nm, typical for 8-aminoxanthine derivatives.[41] The IR showed absorption bands typical for xanthine derivatives.[42]

3. X-ray structure analysis of compounds 8 and 14

Monocrystals suitable for X-ray structural studies were obtained only for 2 of 20 N9-benzyl-substituted pyrimido[2,1-*f*]purinediones. Then the structures of **8** and **14** were determined. In the studied molecules the basic tricyclic pyrimido[2,1-*f*]purinedione is exactly the same (Fig. 4). The purinedione skeleton is coplanar. In the annelated pyrimidine ring three carbon atoms (C6, C7 and C8) possess sp^3 hybridization and this ring in both molecules adopts sofa conformation with the C7 atom in flap position. The C11 atom from substituent at N9 resides in an equatorial position. It is important that C7 and C11 atoms are located on opposite sides of tricycle (*trans* with respect to main skeleton). In the structure of **8** the phenyl attached to C11 is inclined to the pyrimido[2,1-*f*]purinedione at 75.1(1)^0. For the furane ring, placed at C11 in molecule **14**, a respective angle equal to 80.89(7)^0 was found.

The structures of **8** and **14** constituted starting points for subsequent molecular modelling of the molecules described in this study. All molecules contain rotational one atomic-linker (sp^3-hybridized C11), which joins together pyrimido[2,1-*f*]purinedione and the aromatic substituent. Conformational analysis of that molecule

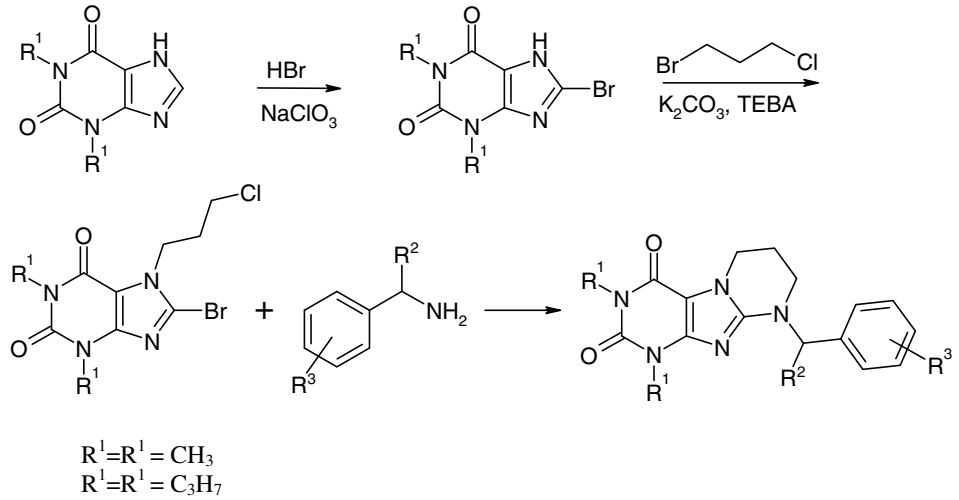

Figure 3. Synthesis of 1,3-dialkyl-9-benzylpyrimido[2,1-*f*]purinediones.

Table 1. Physical data and reaction conditions of 9-benzylpyrimido[2,1-*f*]-purinediones

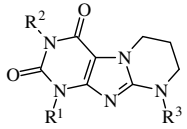

Compound	R^1	R^2	R^3	Mol. form. m.w.	Mp [°C]	Yield [%]	Reaction medium	Reaction time [h]	Crystal. solvent	TLC R_F
1	CH_3	CH_3	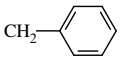	$C_{17}H_{19}O_2N_5$, 325.40	197–198[a]	70	—	3	Ethanol	0.56A
2	CH_3	CH_3	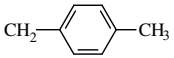	$C_{18}H_{21}O_2N_5$, 339.39	223–224	58	—	4	Ethanol	0.72A
3	CH_3	CH_3	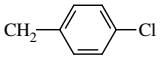	$C_{17}H_{18}O_2N_5Cl$, 359.81	230–232	70	Me-Digol	10	Methoxy-ethanol	0.65A
4	CH_3	CH_3	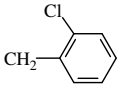	$C_{17}H_{18}O_2N_5Cl$, 359.81	233–235	63	Me-Digol	8	Methoxy-ethanol	0.65A
5	CH_3	CH_3	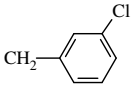	$C_{17}H_{18}O_2N_5Cl$, 359.81	168–169	50	Me-Digol	10	Methoxy-ethanol	0.58A
6	CH_3	CH_3	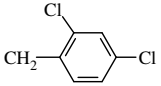	$C_{17}H_{17}O_2N_4Cl_2$, 394.26	195–196	63	Me-Digol	9	*n*-Propanol	0.94A
7	CH_3	CH_3	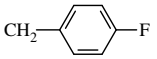	$C_{17}H_{18}O_2N_5F$, 343.35	210–212	40	Me-Digol	8	Methoxy-ethanol	0.58A
8	CH_3	CH_3	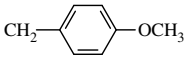	$C_{18}H_{21}O_3N_5$, 355.39	185–187	59	Propanol	3	Propanol	0.63A
9	CH_3	CH_3	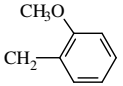	$C_{18}H_{21}O_3N_5$, 355.39	217–218	72	Me-Digol	10	*n*-Butanol	0.68A
10	CH_3	CH_3	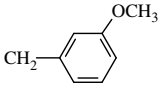	$C_{18}H_{21}O_3N_5$, 355.39	166–167	55	Me-Digol	10	Ethanol	0.64A
11	CH_3	CH_3	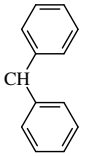	$C_{23}H_{23}O_2N_5$, 401.45	247–249	70	Methoxy-ethanol	10	Propanol	0.74A
12	CH_3	CH_3	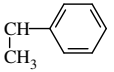	$C_{18}H_{21}O_2N_5$, 339.40	137[a]	80	*n*-Propanol	6	50% Ethanol	0.56A
13	CH_3	CH_3	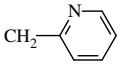	$C_{16}H_{18}O_2N_6$, 326.35	188–190	49	Butanol	6	Isopropanol	0.56B

14	CH_3	CH_3	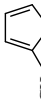	$C_{15}H_{17}O_3N_5$, 315.33	188–189	76	*n*-Propanol	8	Ethanol	0.67A
15			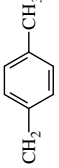	$C_{22}H_{29}O_2N_5$, 395.50	126–128	86	DMF	5	Ethanol/H_2O	0.72C
16			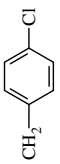	$C_{21}H_{26}O_2N_5Cl$, 415.92	128–130	83	DMF	10	Ethanol/H_2O	0.66C
17			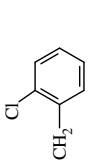	$C_{21}H_{26}O_2N_5Cl$, 415.92	129–132	70	DMF	10	Ethanol/H_2O	0.59C
18			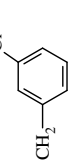	$C_{21}H_{26}O_2N_5Cl$, 415.92	121–124	66	DMF	10	Ethanol/H_2O	0.43C
19			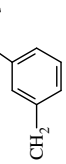	$C_{22}H_{29}O_3N_5$, 422.50	108–110	88	DMF	10	Ethanol/H_2O	0.52C
20			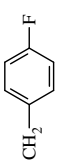	$C_{21}H_{26}O_2N_5F$, 399.47	119–121	70	DMF	10	Ethanol/H_2O	0.49C

TLC A, benzene/acetone 7:3; B, benzene/acetone/methanol 1:1:1; C, toluene/acetone 7:3.
[a] Ref. 38 for compound **1** mp 198.5–200 °C, for compound **12** mp 137 °C.

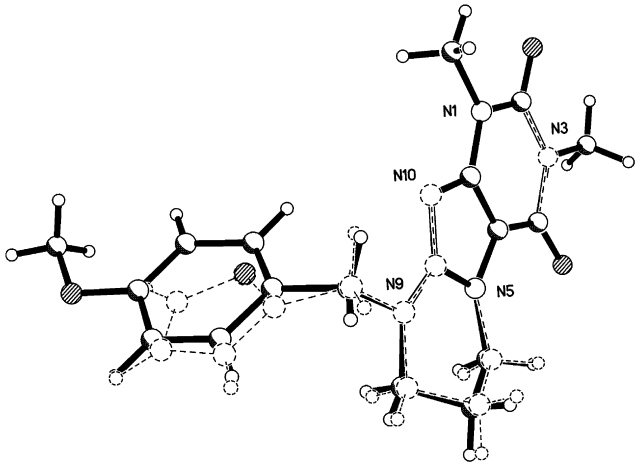

Figure 4. Superimposition of molecules **8** and**14** with respect to pyrimidopurinedione moiety atom.

fragment was performed with Φ = C8–N9–C11–C12 torsion angle rotation.[43] Two energy minima (at $\Phi = \pm 70°$ and ±50° for **8** and **14**, respectively) correspond to *trans* and *cis* location of C7 and C11 atoms with respect to the main molecule skeleton. Conformations present in both studied structures are close to slightly deeper energy minimum describing *trans* form.

In both structures main supramolecular motives are formed by weak intermolecular interactions of O2...H–C8(sp^3) (Table 2b) and (Fig. 5). It should be pointed out that the carbon atom C8 is located as an exact neighbour of the electron-withdrawing non-planar nitrogen N9 (see Table 2a) and that the partial charge on respective hydrogens equals about 0.11e.[44] In the crystals of **8**, due to the 4-OCH_3 substitution of the phenyl ring, an additional weak H-bond of C14–H14...O18 is also observed.

4. Pharmacology

All compounds were tested in vitro in radioligand binding assays for affinity to A_1 and A_{2A} adenosine receptors in rat cortical membrane and rat striatal membrane preparations, respectively. As A_1 AR radioligand [^{3}H]2-chloro-N^6-cyclopentyladenosine ([^{3}H]CCPA) and as A_{2A} receptor ligand [^{3}H]1-propargyl-3-hydroxypropyl-7-methyl-8-(3-methoxystyryl)-xanthine ([^{3}H]MSX-2) were used.[45,46] Selected compounds were additionally investigated at human A_1, A_{2A} and A_3 ARs in mammalian cells recombinantly expressing the respective receptor subtype. As A_3 radioligand we used [^{3}H]2-phenyl-8-ethyl-4-methyl-(8*R*)-4,5,7,8-tetrahydro-1*H*-imidazo[2,1-*i*]purine-5-one ([^{3}H]PSB-11[22]). The results are presented in Table 3. The standard antagonists caffeine (non-selective) and KW-6002 (A_{2A}-selective) were included for comparison.

5. Biological results and discussion

The results of the radioligand binding assays to A_1 and A_{2A} adenosine receptors showed that most of the 1,3-dimethyl-9-benzylpyrimidopurinediones exhibited affinity

Table 2. Selected geometrical data from **8** and **14** molecules

(a) Molecule geometry

	8	**14**
Dihedral angle skeleton/ring at C11 [°]	75.1(1)	80.89(7)
Σ angles at N9 [°]	354.9	358.5
C8–N9–C11–C12 [°]	68.1(2)	56.8(2)

(b) Weak H-bonds in the crystals:

	D–H ... A	Sym. code	D–H (Å)	H ⋯ A (Å)	D ⋯ A (Å)	D–H ⋯ A (°)
8	C8–H8A ⋯ O2	$-1+x, 1+y, z$	1.23	2.17	3.344(3)	158
	C17–H17 ⋯ O18	$-x, 3-y, 1-z$	0.96	2.60	3.354(5)	164
14	C8–H8B⋯O2	$-1+x, y, 1+z$	0.95	2.53	3.458(2)	166

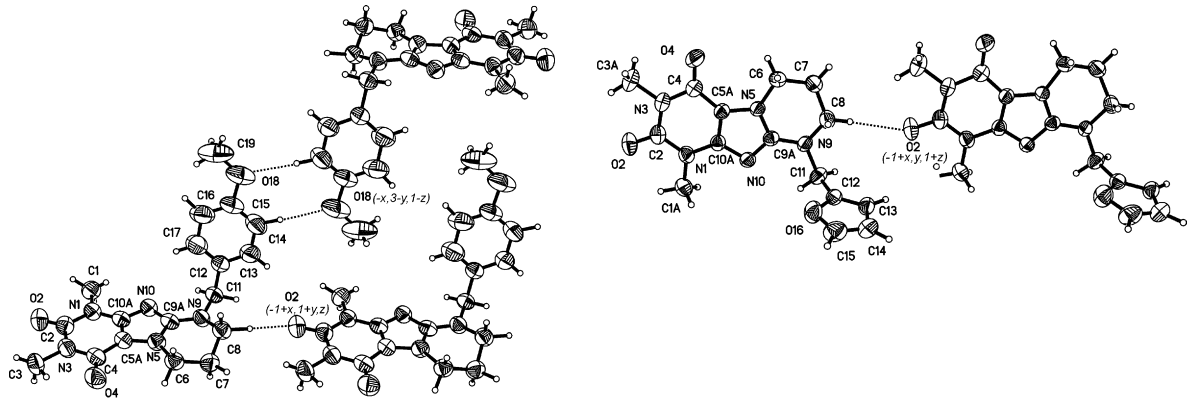

Figure 5. H-bonds net in the crystals of compounds **8** and **14**.

Table 3. Affinities of 9-benzylpyrimido[2,1-*f*]purinediones at A_1 and A_{2A} adenosine receptors

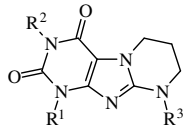

Compound	R^3	A_1[a] versus [^{3}H] CCPA		A_{2A} selectivity A_1/A_{2A}	A_{2A}[b] versus [^{3}H] MSX-2	
		% inhibition at 25 μM (or 2.5 μM)	K_i ± SEM		% inhibition at 25 μM (or 2.5 μM)	K_i ± SEM
Caffeine	—	n.d.[c]	18.8 ± 5.6	—	n.d.[c]	32.5 ± 8.0
KW-6002	Figure 1	n.d.[c]	0.23 ± 0.03		n.d.[c]	0.00515 ± 0.00025
R^1=R^2=CH_3						
1	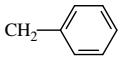	66 ± 3	3.58 ± 0.17	3.28	96 ± 2	1.09 ± 0.30
2	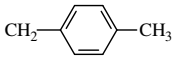	(0)	≫2.5		(26 ± 26)	>2.5
3	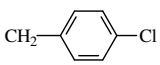	27 ± 5	⩾25		70 ± 9	4.28 ± 0.44
4	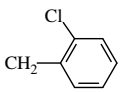	(10 ± 10)	>2.5		(75 ± 4)	1.24 ± 0.20
5	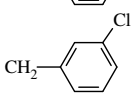	67 ± 1	1.42 ± 0.08		93 ± 4	1.12 ± 0.14

Table 3 (*continued*)

Compound	R^3	A_1[a] versus [^{3}H] CCPA		A_{2A} selectivity A_1/A_{2A}	A_{2A}[b] versus [^{3}H] MSX-2	
		% inhibition at 25 μM (or 2.5 μM)	K_i ± SEM		% inhibition at 25 μM (or 2.5 μM)	K_i ± SEM
6	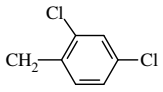	34 ± 11	⩾25		75 ± 7	2.48 ± 0.07
7	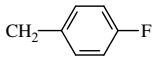	17 ± 10	>25		86 ± 3	2.33 ± 0.21
8	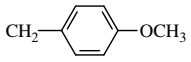	28 ± 2	>25		83 ± 1	5.49 ± 0.54
9	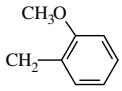	18 ± 6 (11 ± 1)[d]	>25 (>25)[d]		99 ± 1	0.699 ± 0.016 (11.3 ± 2.3)[d]
10	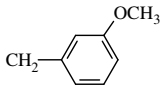	60 ± 7	2.50 ± 0.12	1.9	84 ± 7	1.31 ± 0.13
11	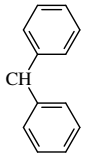	(7 ± 2))	>2.5		(5 ± 5)	>2.5
12	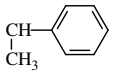	35 ± 8	⩾25	8.8	92 ± 1	2.84 ± 0.17
13[e]	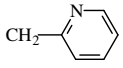	23 ± 4	17.8 ± 0.51	7	79 ± 7	2.53 ± 0.21
14	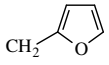	56 ± 1	3.43 ± 0.46		74 ± 4	3.31 ± 0.64
				A_1 selectivity A_{2A}/A_1		
R^1=R^2=C_3H_7						
15	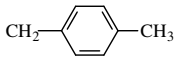	91± 1	1.00 ± 0.15	0.73	60 ± 5(at 3 μM)	0.73 ± 0.09
16[f]	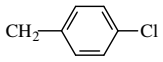	28 ± 1	0.23 ± 0.15	3.6	72. ± 8	0.87 ± 0.41
17	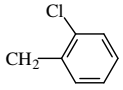	89 ± 3	0.48 ± 0.08	3.6	88 ±1	1.73 ± 0.35
18[g]	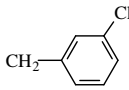	87 ± 31.86 (at 1 μM)	0.089 ± 0.029	14.5	92 ± 2	0.478 ± 0.022
19	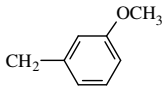	94 ± 1	0.18 ± 0.04	6.28	72 ± 10	1.13 ± 0.14
20	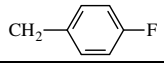	89 ± 1	0.71 ± 0.13	4.8	82 ± 10	3.43 ± 0.71

[a] Rat brain cortical membranes.
[b] Rat brain striatal membranes.
[c] n.d., not determined.
[d] Data from human recombinant receptors permanently expressed in CHO cells.
[e] K_i value of **13** at human A_3 ARs ≫ 10 μM (4% inhibition of radioligand binding at 10 μM).
[f] K_i value of **16** at human A_3 ARs: 1.60 ± 0.30 μM.
[g] K_i value of **18** at human A_3 ARs: 1.29 ± 0.31 μM.

to A_{2A} receptors but poor A_1 affinity (Table 3). The lead structure benzylpyrimidopurinedione (**1**) showed affinity for A_1 and A_{2A} receptors in the low micromolar concentration range with 3-fold A_{2A} selectivity (K_iA_{2A} = 1.09 μM, (K_iA_1 = 3.58 μM). Introduction of substituents R^3 (CH_3, OCH_3, Cl, F) in the *p*-position of the benzyl residue was disadvantageous for A_{2A} affinity (e.g., **2**, **3**, **7**, **8**). Better tolerated were substituents in the *m*- or *o*-position. The *o*-methoxy derivative **9** was the best A_{2A} ligand (K_i = 0.699 μM) of the presented series.

Introduction of a substituent R^2 at the methylene linker of the benzyl residue (methyl in **12**, phenyl in **11**) was disadvantageous too. The phenyl substituent (**11**) decreased affinity to both kinds of receptors practically to zero (5% and 7% inhibition of radioligand binding at 2.5 μM). The isosteric exchange of the phenyl ring (in the 9-benzyl substituent) by a heterocyclic ring (furyl in **14**, pyridyl in **13**) had the similar effect. Taking into account previously described results[33] on the arylpyrimidopurinediones (**II**), examined for the profile at A_{2A} activity in sodium chloride shift experiments, it might be suggested that recently investigated compounds also exhibit A_{2A} antagonistic activity.[47]

The most interesting effects were observed in compounds showing an elongation of the substituents in the 1- and 3-positions from methyl to propyl (compounds **15**–**20**). Affinity to both kinds of receptors increased, however A_1 affinity increased to a larger extent, with the result that A_{2A} selectivity was abolished (compound **15**). All investigated dipropyl-substituted compounds showed submicromolar A_1 affinity (with the exception of **15**, K_i = 1.00 μM). The best A_1 ligand was compound **18** (K_i = 0.089 μM and 5-fold A_1 selectivity).

The most potent and at the same time most selective compound **9** was additionally tested at human A_1 and A_{2A} receptors to investigate possible species differences. In fact, **9** exhibited lower affinity for the human than for the rat receptors: its K_i value at the human A_{2A} receptor (K_i = 11.3 μM) was 16-fold lower than that at the rat receptor (K_i = 0.699 μM). The same tendency, lower affinity for human than for rat A_{2A} receptors, has been observed for other members of the pyrimido[2,1-*f*]purinedione family.[35] Three selected compounds were investigated at human A_3 ARs, one dimethyl derivative (**13**) and two dipropyl derivatives (**16**, **18**). While the dimethyl derivative was inactive at A_3 receptors, the dipropyl derivatives exhibited K_i values of 1–2 μM. This result is in accordance with data from bicyclic xanthine derivatives, in which a dipropyl substitution is very favourable for A_3 affinity, in contrast to a dimethyl substitution.[21,48] It can be concluded that the *N*,*N*-dipropyl substitution of the xanthine part is not only unfavourable for A_{2A}-selectivity versus A_1, but also versus A_3 ARs.

6. Structure–activity relationships

Starting with structure–activity relationship analysis, the K_i values of pyrimido[2,1-*f*]purinedione of both studied receptors (A_1 and A_{2A}) were examined as a function of the calculated lipophilicity descriptor, log *P* (and log *D*).[49] All indispensable numerical data are collected in Table 4 while results in graphical forms are presented in Figures 6 and 7. After primary analysis two series of derivatives were selected: one with R^1=CH_3 (compounds **1**–**14**) and the other one with R^1=C_3H_7 (compounds **15**–**20**). This is in accordance with two clusters observed on the diagrams of K_i value versus log *P* (Figs. 6 and 7). Two linear relationships—involving log *P* for both series of compounds and affinity to A_1 receptor (K_i A_1 values on Fig. 7)—were shown. Linear equations make it impossible to estimate the optimal values of

Table 4. Physicochemical, geometrical and electronic parameters of studied pyrimido[2,1-*f*]purinediones considered in QSAR studies

	Pharmacological data		Lipophilicity		Geometrical data		QSAR			Electronic parameters	
	K_i A_1	K_i A_{2A}	log *P*	log *D*	*V* A_3	d*V*	MR	MP	Hyd. en	HOMO	DP
1	3.58	1.09	1.50	1.12	920.06	202.28	89.06	37.17	−0.84	−8.44	5.328
2			1.93	1.53	972.03	254.25	94.10	39.00	0.32	−8.42	5.502
3		4.28	2.22	1.96	963.04	245.26	93.86	39.10	−0.51	−8.51	4.881
4		1.24	2.21	1.95	951.57	233.79	93.86	39.10	−0.64	−8.46	4.576
5	1.42	1.12	2.28	2.02	958.87		93.86	39.10	−0.39	−8.49	4.227
6		2.48	3.00	2.83	994.44	276.62	98.67	41.02	−0.33	−8.53	4.037
7		2.33	1.65	1.38	929.30	211.52	89.27	37.08	−0.55	−8.51	4.894
8		5.49	1.45	1.11	997.83	280.05	95.52	39.64	−2.52	−8.41	4.420
9		0.70	1.46	1.12	992.26	274.48	95.52	39.64	1.09	−8.34	6.775
10	2.5	1.31	1.56	1.22	996.26	279.15	95.52	39.64	−2.35	−8.42	5.448
11			3.18	2.90	1103.95	386.17	113.34	46.83	−1.46	−8.39	5.266
12		2.84	2.03	1.76	960.72	291.31	93.48	39.00	−0.38	−8.40	5.449
13	17.8	2.53	0.40	0.32	962.10	244.32	86.50	37.13	−1.03	−8.31	6.876
14	3.43	3.31	0.90	0.71	879.32	161.54	81.45	31.90	−3.33	−8.43	5.777
15	1.00	0.73	2.86	2.42	1168.71		112.64	46.34	−1.54	−8.36	5.090
16	0.23	0.87	4.17	3.93	1159.92	235.30	112.41	46.44	0.73	−8.44	4.730
17	0.48	1.73	4.16	3.92	1147.89	223.45	112.41	46.44	0.57	−8.39	4.099
18	0.089	1.29	4.22	3.99	1159.02		112.41	46.44	0.68	−8.45	3.820
19	0.18	1.13	3.40	3.08	1193.65	274.20	114.06	46.98	−1.30	−8.35	6.153
20	0.71	3.43	3.59	3.35	1125.25	201.94	107.82	44.42	0.65	−8.45	4.777

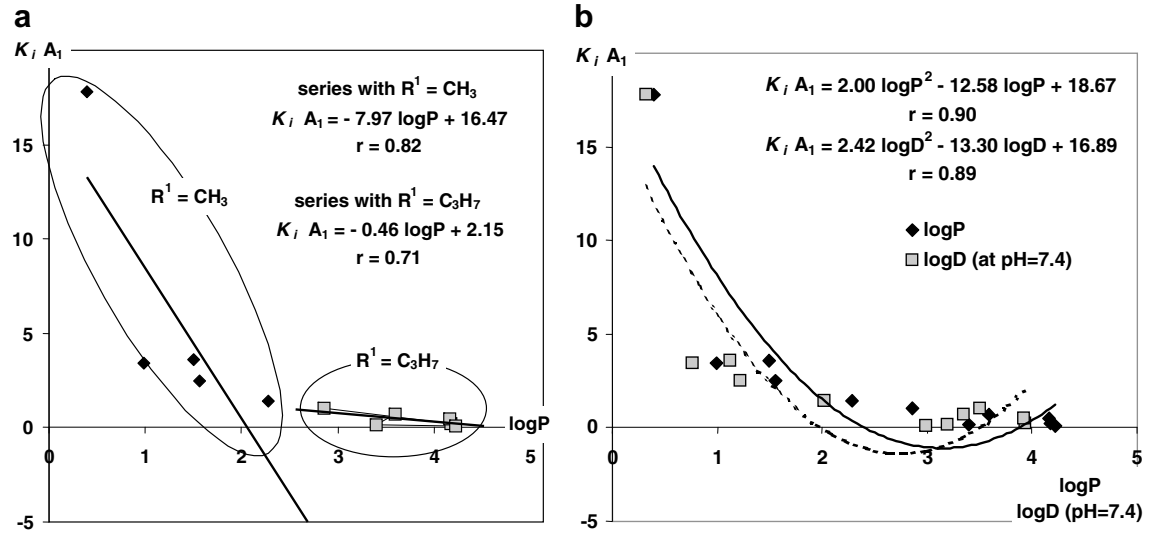

Figure 6. Relationships of K_i to A_1 receptor in the function of log *P* for two series of derivatives with identical R^1 substituents.

log *P*. Considering both series as one group, the second degree polynominal equation between log *P* and K_i for A_1 enables to evaluate the optimal value of lipophilicity for pyrimido[2,1-*f*]purinediones. This optimum was found at about 3 for log *P* and log *D* (at pH 7.4) (Fig. 6b). Contrary to the above, the relationships between log *P* and the activity towards adenosine A_{2A} receptor (K_i for A_{2A} values in Fig. 7) are not obvious. It means that lipophilicity for the activity for adenosine A_{2A} receptor is less significant than that to A_1 receptor. In Table 4 also some other similarity descriptors—geometrical and electronic ones—are collected for studied pyrimido[2,1-*f*]purinediones. Unfortunately, no explicit conclusions could have been drawn based on one or multilinear relationships.[50]

6.1. Benzylpyrimido[2,1-*f*]purinediones and A_1 receptor interactions

The relationships of $K_i = f$ (log *P* and/or log *D*) pointed out an importance of lipophilicity for activity of the benzylpyrimido[2,1-*f*]purinediones to A_1 receptor (Fig. 6) but not to A_{2A} one (Fig. 7). The impact of lipophilicity for A_1 receptor ligands is manifested also in the appropriate pharmacophore model which consists of as many as three lipophilic pockets essential for ligand–receptor interactions.[51,52] Besides these, two H-bond acceptors and one H-bond donor are needed for binding. Keeping this in mind, that model has been adopted to benzylpyrimido[2,1-*f*]purinedione molecules in the manner depicted on Figure 8.

Two R^1 substituents from the studied benzylpyrimido[2,1-*f*]purinediones are located in the lipophilic pockets P2 and P3. In accordance with the data from Tables 3 and 4, replacement of both R^1=CH_3 by C_3H_7 increases log *P* value as well as molecule activity for adenosine A_1 receptor. Thus, two three-atomic chains more efficiently fix the molecule at the respective binding site of the receptor. Furthermore, purine oxygen—located between R^1 substituents—is shielded by spaces occupied by the propyl chains. In consequence, as it was observed in

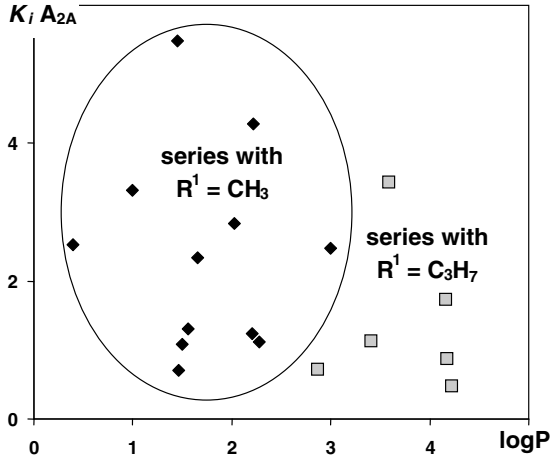

Figure 7. Relationships of K_i to A_{2A} receptor with log *P* values.

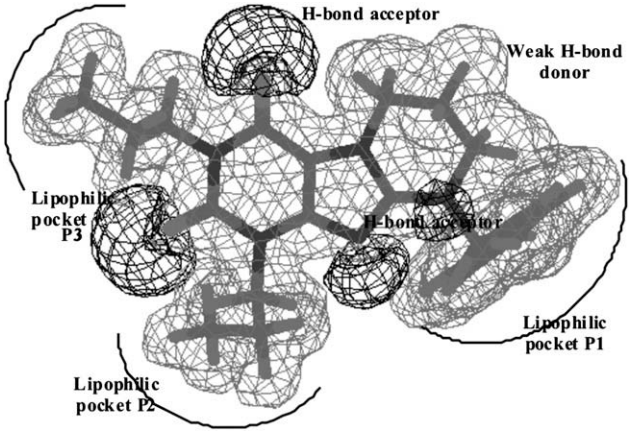

Figure 8. Model of interaction of benzylpyrimido[2,1-*f*]purinediones with A_1 receptor.

Table 5. Spectroscopic data of compounds **1**–**20**

Compound	UV [nm]	IR [cm^{-1}]	^1H NMR
1	299[38]	1704 CO (pos. 2) 1654 CO (pos. 4)	2.11–2.18 (m, 2H, CH_2CH_2–CH_2), 3.18 (t, 2H, J = 5.54 Hz, CH_2N_9), 3.41 (s, 3H, N_3CH_3), 3.56 (s, 3H, N_1CH_3), 4.26 (t, 2H, J = 6.05 Hz, N_5CH_2), 4.78 (s, 2H, N_9CH_2), 7.30–7.41 (m, 5H, phenyl)
2	301	1704 CO (pos. 2) 1657 CO (pos. 4)	2.07–2.13 (m, 2H, CH_2–CH_2CH_2), 2.34 (s, 3H, CH_3), 3.26 (t, 2H, J = 5.78 Hz, CH_2N_9), 3.36 (s, 3H, N_3CH_3), 3.52 (s, 3H, N_1CH_3), 4.21 (t, 2H, J = 6.02 Hz, N_5CH_2), 4.70 (s, 2H, N_9CH_2), 7.12–7.23 (m, 4H, phenyl)
3	301	1697 CO (pos. 2) 1655 CO (pos. 4)	2.08–2.17 (m, 2H, CH_2–CH_2CH_2), 3.24–3.27 (m, 2H, CH_2N_9), 3.37 (s, 3H, N_3CH_3), 3.52 (s, 3H, N_1CH_3), 4.23 (t, 2H, J = 6.00 Hz, N_5CH_2), 4.71 (s, 2H, N_9CH_2), 7.24–7.34 (m, 4H, phenyl)
4	302	2705 CO (pos. 2) 1651 CO (pos. 4)	2.16–2.23 (m, 2H, CH_2–CH_2CH_2), 3.36 (t, 2H, J = 5.64 Hz, CH_2N_9), 3.41 (s, 3H, N_3CH_3), 3.54 (s, 3H, N_1CH_3), 4.29 (t, 2H, J = 6.05 Hz, N_5CH_2), 4.92 (s, 2H, CH_2N_9), 7.26–7.32 (m, 2H, H4,5-phenyl), 7.39–7.45 (m, 2H, H3,6-phenyl)
5	301	1691 CO (pos. 2) 1660 CO (pos. 4)	2.14–2.22 (m, 2H, CH_2–CH_2CH_2), 3.30 (t, 2H, J = 5.64 Hz, CH_2N_9), 3.41 (s, 3H, N_3CH_3), 3.56 (s, 3H, N_1CH_3), 4.27 (t, 2H, J = 5.91 Hz, N_5CH_2), 4.75 (s, 2H, N_9CH_2), 7.21–7.25 (m, 1H, H2-phenyl), 7.31–7.34 (m, 3H, H4,5,6-phenyl)
6	301	1702 CO (pos. 2) 1654 CO (pos. 4)	2.12–2.21 (m, 2H, $CH_2CH_2CH_2$), 3.31–3.37 (m, 5H, N_3CH_3 + CH_2N_9), 3.50 (s, 3H, N_1CH_3), 4.25 (s, 2H, J = 6.23 Hz, N_5CH_2), 4.83 (s, 2H, N_9CH_2), 7.21–7.43 (m, 3H, phenyl)
7	304	1702 CO (pos. 2) 1662 CO (pos. 4)	2.07–2.17 (m, 2H, CH_2–CH_2CH_2), 3.24 (t, 2H, J = 5.00 Hz, CH_2N_9), 3.38 (s, 3H, N_3CH_3), 3.53 (s, 3H, N_1CH_3), 4.22 (t, 2H, J = 6.25 Hz, N_5CH_2), 4.70 (s, 2H, N_9CH_2), 7.00–7.07 (m, 2H, H2,6-phenyl), 7.27–7.32 (m, 2H, H3,5-phenyl)
8	301	1697 CO (pos. 2) 1656 CO (pos. 4)	2.05–2.15 (m, 2H, $CH_2CH_2CH_2$), 3.23 (t, 2H, J = 5.38 Hz, CH_2N_9), 3.38 (s, 3H, N_3CH_3), 3.53 (s, 3H, N_1CH_3), 3.80 (s, 3H, OCH_3), 4.21 (t, 2H, N_5CH_2), 4.67 (s, 2H, N_9CH_2), 6.86–6.90 (m, 2H, H3,5-phenyl), 7.23–7.27 (m, 2H, H2,6-phenyl)
9	300	1702 CO (pos. 2) 1651 CO (pos. 4)	2.07–2.17 (m, 2H, CH_2–CH_2–CH_2), 3.05–3.37 (m, 5H, N_3CH_3, CH_2N_9), 3.52 (s, 3H, N_1CH_3), 3.84 (s, 3H, OCH_3), 4.22 (t, 2H, J = 6.25 Hz, N_5CH_2), 4.76 (s, 2H, N_9CH_2), 6.88–6.96 (m, 2H, H4,5-phenyl), 7.25–7.31 (m, 2H, H3,6-phenyl)
10	302	1698 CO (pos. 2) 1653 CO (pos. 4)	2.07–2.10 (m, CH_2–CH_2–CH_2), 3.27 (t, 2H, J = 5.65 Hz, CH_2N_9), 3.68 (s, 3H, N_3CH_3), 3.51 (s, 3H, N_1CH_3), 3.79 (s, 3H, OCH_3), 4.32 (t, 2H, J = 6.02 Hz, N_5CH_2), 4.71 (s, 2H, N_9CH_2), 6.91–6.97 (m, 2H, H4,5-phenyl), 7.22–7.30 (m, 2H, H2,6-phenyl)
11	299	1700 CO (pos. 2) 1648 CO (pos. 4)	2.10–2.19 (m, 2H, CH_2–CH_2_CH_2), 3.15 (t, 2H, J = 5.88 Hz, CH_2N_9), 3.35 (s, 3H, N_3CH_3), 3.51 (s, 3H, N_1CH_3), 4.21 (t, 2H, J = 6.01 Hz, N_5CH_2), 7.06 (s, 1H, CH), 7.25–7.38 (m, 10H, phenyl)
12	299[15]	1690 CO (pos. 2) 1659 CO (pos. 4)	1.63 (t, 3H, J = 6.25 Hz), 1.94–2.07 (m, 2H, CH_2N_9), 2.91–3.02 (m, 1H, CH_2N_9), 3.17–3.26 (m, 1H, CH_2N_9), 3.38 (s, 3H, N_3CH_3), 3.54 (s, 3H, N_1CH_3), 4.13–4.27 (m, 2H, N_5CH_2), 5.83–5.91 (q, J = 7.5 Hz, 1H, N_9–CH), 7.26–7.37 (m, 5H, phenyl)
13	299	1703 CO (pos. 2) 1654 CO (pos. 4)	2.11–2.21 CH_2–CH_2–CH_2), 3.37–3.45 (m, 5H, N_3CH_3 + CH_2N_9), 3.50 (s, 3H, N_1CH_3), 4.25 (t, 2H, J = 6.00 Hz, N_5CH_2), 4.86 (s, 2H, N_9CH_2), 7.25–7.36 (m, 2H, H3,5-pyridyl), 7.65–7.71 (td, 1H, H4-pyridyl), 8.56–8.58 (m, 1H, H6-pyridyl)
14	302	3100 furan 1700 CO (pos. 2) 1652 CO (pos. 4)	2.09–2.18 (m, 2H, $CH_2CH_2CH_2$), 3.31–3.36 (m, 5H, N_3CH_3, CH_2N_9), 3.53 (s, 3H, N_1CH_3), 4.24 (t, 2H, J = 6.00 Hz, N_5CH_3), 4.71 (s, 2H, N_9CH_2), 6.30–6.35 (m, 2H, H3,4-furyl), 7.38 (s, 1H, H5-furyl)

15	300	1687 CO (pos. 2) 1654 CO (pos. 4)	0.92–0.98 (m, 6H, 2 $CH_3CH_2CH_2$), 1.57–1.82 (m, 6H, 2 CH_3–CH_2 + H_2O), 2.06–2.13 (m, 2H, N_5CH_2–CH_2–CH_2N_9), 2.34 (s, 3H, CH_3 phenyl), 3.23 (t, 2H, J = 5.77 Hz, CH_2N_9), 3.91–4.03 (m, 4H, N_1, N_3, CH_2CH_2–CH_3), 4.20 (t, 2H, J = 6.05 Hz, N_9CH_2), 7.13–7.23 (m, 4H, phenyl)
16	302	1686 CO (pos. 2) 1653 CO (pos. 4)	0.92–0.98 (m, 6H, 2 CH_3CH_2–CH_2), 1.55–1.83 (m, 6H, 2 CH_2–CH_2CH_3 + H_2O), 2.08–2.16 (m, 2H, N_5–CH_2–CH_2CH_2–N_9), 3.24 (t, 2H, J = 5.64 Hz, CH_2N_9), 3.94–4.02 (m, 4H, N_1, N_3, CH_2–CH_2–CH_3), 4.22 (t, 2H, J = 6.05 Hz, N_5CH_2), 4.68 (s, 2H, N_9CH_2), 7.24–7.32 (m, 4H, phenyl)
17	300	1694 CO (pos. 2) 1654 CO (pos. 4)	0.91–0.97 (m, 6H, 2 CH_3–CH_2CH_2), 1.56–1.81 (m, 4H, 2 CH_3CH_2–CH_2), 2.11–2.19 (m, 2H, N_5–CH_2–CH_2–CH_2–N_9), 3.32–3.57 (m, 2H, CH_2N_9), 3.91–4.01 (m, 4H, N_1, N_3, CH_2–CH_2CH_3), 4.24 (t, 2H, J = 6.05 Hz, N_5CH_2), 4.86 (s, 2H, N_9CH_2), 7.22–7.26 (m, 2H, H4,5-phenyl), 7.38–7.41 (m, 2H, H3,6-phenyl)
18	302	1695 CO (pos. 2) 1653 CO (pos. 4)	0.92–0.98 (m, 6H, 2 $CH_3CH_2CH_2$), 1.59–1.84 (m, 4H, 2 CH_3–CH_2CH_2), 2.10–2.17 (m, 2H, N_5CH_2–$CH_2CH_2N_9$), 3.25–3.50 (m, 2H, CH_2N_9), 3.91–4.03 (m, 4 H, N_1, N_3, $CH_2CH_2CH_3$), 4.42 (t, 2H, J = 6.05 Hz, N_5CH_2), 4.68 (s, 2H, N_9CH_2), 7.18–7.34 (m, 4H, phenyl)
19	300	1698 CO (pos. 2) 1653 CO (pos. 4)	0.92–0.97 (m, 6H, 2 $CH_3CH_2CH_2$), 1.60–1.81 (m, 4H, 2 CH_3–CH_2CH_2), 2.07–2.15 (m, 2H, N_5CH_2–$CH_2CH_2N_9$), 3.25 (t, 2H, J = 5.78 Hz, CH_2N_9), 3.79 (s, 3H, OCH_3), 3.91–4.02 (m, 4H, N_1, N_3, $CH_2CH_2CH_3$), 4.21 (t, 2H, J = 6.05 Hz, N_5CH_2), 4.68 (s, 2H, N_9CH_2), 6.81–6.90 (m, 3H, H4,5,6-phenyl), 7.23–7.28 (m, 1H, H2-phenyl)
20	302	1686 CO (pos. 2) 1654 CO (pos. 4)	0.92–0.98 (m, 6H, 2 CH_3–CH_2–CH_2), 1.60–1.84 (m, 6H, 2 CH_2–CH_2–CH_3 + H_2O), 2.07–2.15 (m, 2H, N_5CH_2–$CH_2CH_2N_9$), 3.24 (t, 2H, J = 5.64 Hz, CH_2N_9), 3.91–4.03 (m, 4H, N_1, N_3, $CH_2CH_2CH_3$), 4.21 (t, 2H, J = 6.05 Hz, N_5CH_2) 4.68 (s, 2H, N_9CH_2), 6.98–7.06 (m, 2H, H2,6-phenyl), 7.26–7.32 (m, 2H, H3,5-phenyl)

the structure of 1,3-dipropyl-arylpyrimido[2,1-*f*]purinedione, that oxygen is going to be not effective as H-bond acceptor.[33] Aromatic substituent located at N9-nitrogen is filling the third lipophilic area, marked as P1 in Figure 8. It is essential that replacement of phenyl by heterocycles (pyridyl or furane in compounds **13** and **14**, respectively) decreases the activity of the compound. We suppose that the properties and capacity of P1 pocket should be studied more intensively on the base of pyrimido[2,1-*f*]purinediones with a variety of spacers joining aromatic group with the main skeleton.

Beside lipophilic pockets, the model in Figure 8 consists of two H-bond acceptors: one at the not protected purine oxygen and the second one at the imidazole nitrogen. Reference pharmacophore model for ligands of A_1 receptor comprises also H-bond donor, it should be located in the proximity of tetrahydropyrimidine ring. H-Bond donor in this area of the molecule was detected in the crystal structure of **8** and **14** (see above). It involves endocyclic tetrahydropyrimidine carbon atom (C8) with hydrogens of higher acidity to form C–H...O weak interaction (Fig. 5).

7. Conclusions

A series of 20 new benzyl derivatives of pyrimido[2,1-*f*]purinediones was obtained. The new compounds were tested for their adenosine receptor affinity. 1,3-Dimethyl derivatives exhibited adenosine A_{2A} receptor selectivity and affinity at micromolar and submicromolar concentrations. 1,3-Dipropylbenzylpyrimidopurinediones have shown submicromolar affinity and selectivity towards A_1 AR. *p*-Substituents of the benzyl residues, substituent R^2 at the methyl linker and isosteric exchange of the phenyl moiety were disadvantageous for A_1 and A_{2A} adenosine receptor activity. SAR studies have revealed dependence between A_1 AR affinity and log *P* value. Pharmacophore model for A_1 R ligands has been created.

8. Experimental

8.1. Chemistry

Melting points were determined on a MEL-TEMP II apparatus and are uncorrected. IR spectra were recorded as KBr discs on a FT Jasco IR 410 spectrometer. ^{1}H NMR spectra were recorded on a Varian-Mercury 300 MHz (compounds **1**, **4**, **5**, **15**–**20**) or Bruker VM 250 (compounds **3**, **6**–**9, 11**–**14**) or Bruker Ac 200F (compounds **2**, **10**) spectrometer in $CDCl_3$, using TMS as an internal standard. UV spectra were recorded on a Jasco UV/VIS V-530 apparatus in concentration 10^{-5} mol/L in methanol (Table 9). Elemental analyses (C, H, N) were within ±0.4% of theoretical values and were performed on an Elemental-Vario-EL III apparatus.

TLC data were obtained with Merck-Silica gel $60F_{254}$ aluminium sheets, using benzene/acetone 7:3 (A), benzene/acetone/methanol 3:3:3 (B) and toluene/acetone

Table 6. Reaction conditions and yields of 1,3-dipropyl-9-benzylpyrimido[2,1-*f*]-purinediones obtained by microwave method

Compound	Reaction time [min]	Microwave power [W]	Yield[%]
15	5	450	85
16	10	750	82
17	7	450	85
18	10	450	90
19	4	300	87
20	10	450	98

7:3 (C) as developing systems. The plates were visualized with UV light.

8.1.1. General procedure for the synthesis of 9-benzyl 1, 3-dimethyl-6,7,8,9-tetrahydro pyrimido[2,1-*f*]purine-2,4 (1H,3H)-dione (1–14). A mixture of 0.66 g (2 mmol) of 7-(3-chloropropylo)-8-bromotheophylline[37] and corresponding amine (4–30 mmol) was refluxed in appropriate solvent (propanol, butanol, methoxyethanol, Me-Digol)) or without solvent for 4–10 h (see Table 1). After cooling the precipitate was separated, washed with ethanol and water. All compounds were purified by crystallization (see Table 1).

8.1.2. General procedure for the synthesis of 9-benzyl 1, 3-dipropyl-6,7,8,9-tetrahydro pyrimido[2,1-*f*]purine-(1H, 3H)-dione (15–20). Starting materials.

8.1.2.1. 8-bromo-1,3-dipropylxanthine. A mixture of 12.15 g (50 mmol) of 1,3-dipropylxanthine,[39,40] 39 ml acetic acid and 6.8 ml (75 mmol) of 40% HBr was stirred at 50 °C until dissolution was completed. The temperature was raised to 58 °C and the solution of 2.04 g (18 mmol) $NaClO_3$ in 14.4 ml of water was added dropwise during 1 h.

Heating and stirring was continued lasting for 2 h. The white solid precipitated, which was filtered off on the next day, washed with cold water, hot water and ethanol.

The yield 78%, mp 179–182 °C.

Spectral data:

UV: λ_{max} = 279 nm.

IR [cm^{-1}]: 3063 (NH), 2965–2874 (–CH_2), 1705 [–CO (pos. 2)], 1660 [–CO (pos. 4)], 760 (–CH_2).

^1H NMR ($CDCl_3$) δ: 0.95–1.01 (m, 6H, $CH_2CH_2CH_3$); 1.68–1.88 (m, 4H, $CH_2CH_2CH_3$); 4.04–4.10 (m, 4H, $CH_2CH_2CH_3$); 13.55 (s, 1H, NH).

8.1.2.2. 1,3-dipropylo-7-(3-chloropropyl)-8-bromoxanthine. A mixture of 15.3 g (24 mmol) of 1,3-dipropyl-8-bromoxanthine, 5.92 g (43 mmol) of anhydrous K_2CO_3, 7.88 ml (80 mmol) of 1-bromo-3-chloropropane, 0.49 g (2 mmol) of TEBA and 150 ml of acetone was refluxed for 10 h with stirring. The unreacted 1, 3-dipropyl-8-bromoxanthine and inorganic salts were filtered off from the hot mixture. This precipitate contained also a small amount of the main product. The acetone filtrate was cooled overnight. The precipitated product was separated. To remove unreacted 1,3-dipropyl-8-bromoxanthine these two crops of product were stirred at room temperature with 5% NaOH, filtered off and washed with water.

Table 7. Crystal data and structure refinement details for **8** and **14**

	8	**14**
Empirical formula	$C_{18}H_{21}N_5O_3$	$C_{15}H_{17}N_5O_3$
Formula weight	355.40	315.33
Temperature	293(2) K	293(2) K
Wavelength	1.54178 Å	0.71073 Å
Crystal system	Triclinic	Monoclinic
Space group	P-1	$P2_1/n$
Unit cell dimensions	a = 5.0020(10) Å	a = 5.1665(8) Å
	b = 9.653(2) Å	b = 30.497(4) Å
	c = 17.745(4) Å	c = 9.6592(13) Å
	α = 91.99(3)°	
	β = 92.18(3)°	β = 94.56(1)°
	γ = 91.52(3)°	
Volume	855.3(3) $Å^3$	1503.0(4)
Z, Calculated density	2, 1.380 Mg/m^3	4, 1.394 Mg/m^3
Absorption coefficient	0.797 mm^{-1}	0.101 mm^{-1}
F(000)	376	664
Crystal size	0.1 × 0.1 × 0.4 mm	0.25 × 0.3 × 0.5 mm
Theta range for data index	2.5–80.0°	2.52–25°
Ranges	−6:h:6, −12:k:12, 0:l:22	−5:h:6, −36:k:36, −11:l:11
Diffractometer	KM-4	KM-4 with CCD detector
Refl. collected/unique	7098/3549 [R(int) = 0.107]	16,079/2647 [R(int) = 0.028]
Refinement method	Full-matrix-block least-squares on F^2	Full-matrix-block least-squares on F^2
Data/parameters	3549/242	2647/212
Goodness-of-fit on F^2	0.91	1.06
Final R [$I > 2\sigma(I)$]	$R1$ = 0.0643, $wR2$ = 0.1291	$R1$ = 0.0361, $wR2$ = 0.1078
Largest diff. peak and hole	0.30 and −0.32 e $Å^{-3}$	0.17 and −0.16 e $Å^{-3}$

Table 8. Atomic coordinates ($\times 10^4$) and equivalent isotropic displacement parameters ($\text{Å}^2 \times 10^3$) for **8** and **14**

		8		
O2	0.4882(5)	0.4127(2)	0.19775(13)	0.0769(9)
O4	0.6224(5)	0.7831(3)	0.04895(13)	0.0830(9)
O18	0.2069(7)	1.3238(3)	0.53674(15)	0.1190(2)
N1	0.2545(5)	0.6036(2)	0.22333(13)	0.0563(8)
N3	0.5524(5)	0.5976(3)	0.12334(14)	0.0631(9)
N5	0.2028(5)	0.9300(2)	0.14438(12)	0.0555(8)
N9	−0.1235(5)	1.0453(2)	0.21194(12)	0.0562(8)
N10	0.0137(5)	0.8153(2)	0.23758(13)	0.0558(8)
C1A	0.1162(7)	0.5372(3)	0.28392(17)	0.0692(9)
C2	0.4339(6)	0.5308(3)	0.18332(18)	0.0618(9)
C3A	0.7419(7)	0.5185(4)	0.08060(18)	0.0778(9)
C4	0.5031(6)	0.7341(3)	0.10225(16)	0.0602(9)
C5A	0.3139(6)	0.7985(3)	0.14664(15)	0.0558(9)
C6	0.2644(6)	1.0440(3)	0.09553(16)	0.0617(9)
		14		
O2	0.9957(5)	0.11487(10)	0.3774(2)	0.0634(10)
O4	1.1365(5)	0.02913(9)	0.7744(3)	0.0647(10)
O16	0.5151(5)	0.22594(9)	1.0728(3)	0.0674(10)
N1	0.7593(5)	0.13134(9)	0.5629(3)	0.0455(10)
N3	1.0592(5)	0.07217(9)	0.5757(3)	0.0464(10)
N5	0.7185(5)	0.08714(8)	0.9026(3)	0.0371(8)
N9	0.3916(5)	0.12808(9)	1.0033(3)	0.0451(9)
N10	0.5225(5)	0.14169(8)	0.7710(3)	0.0412(9)
C1A	0.6218(8)	0.16754(12)	0.4864(4)	0.0582(14)
C2	0.9410(6)	0.10686(12)	0.4981(3)	0.0466(12)
C3A	1.2505(7)	0.04603(14)	0.5039(4)	0.0633(16)
C4	1.0168(6)	0.06021(11)	0.7166(3)	0.0449(12)
C5A	0.8277(6)	0.08712(10)	0.7717(3)	0.0384(10)
C6	0.7669(7)	0.05672(11)	1.0214(4)	0.0468(12)
C7	0.5336(7)	0.05825(12)	1.1085(4)	0.0538(12)
C8	0.4559(7)	0.10537(12)	1.1365(3)	0.0497(11)
C9A	0.5381(6)	0.11997(10)	0.8947(3)	0.0378(10)
C10A	0.7035(6)	0.12081(10)	0.6979(3)	0.0389(11)
C11	0.2136(7)	0.16588(11)	0.9989(4)	0.0488(12)
C12	0.2984(6)	0.20180(10)	1.0982(3)	0.0420(11)
C13	0.2031(7)	0.21669(11)	1.2151(4)	0.0482(12)
C14	0.3641(8)	0.25200(13)	1.2678(4)	0.0602(14)
C15	0.5477(8)	0.25645(13)	1.1803(5)	0.0697(16)

U_{eq} is defined as one-third of the trace of the orthogonalized U_{ij} tensor.

Table 9. Elemental analysis

Compound		Analyses [%]		
		C	H	N
1	Ref. 6	62.76	5.89	21.53
		62.65	6.15	21.52
2		63.71	6.24	20.64
		63.44	6.15	20.96
3		56.75	5.05	19.46
		56.59	4.87	19.28
4		56.75	5.05	19.46
		56.83	5.06	19.26
5		56.75	5.05	19.46
		56.52	5.23	19.61
6		51.79	4.35	17.77
		51.66	4.08	17.53
7		59.46	5.29	20.40
		59.35	5.05	20.39
8		60.83	5.96	19.71
		60.64	5.85	19.48
9		60.83	5.96	19.71
		60.46	5.84	19.90
10		60.83	5.96	19.71
		61.09	5.64	19.46
11		68.80	5.78	17.44
		68.80	5.50	17.21
12	Ref. 6	63.69	6.24	20.64
		63.76	6.62	20.72
13		58.90	5.57	25.75
		58.93	5.74	26.10
14		57.14	5.44	22.21
		57.20	5.33	22.22
15		66.83	7.40	17.71
		66.63	7.44	17.40
16		60.64	6.31	16.83
		60.53	6.32	16.53
17		60.64	6.31	16.83
		60.83	6.29	16.93
18		60.64	6.31	16.83
		60.74	6.31	16.52
19		64.22	7.11	17.02
		64.10	7.19	17.00
20		63.14	6.57	17.53
		62.85	6.55	17.50

Spectral data:

UV: λ_{max} = 279.5 nm.

IR [cm^{-1}]: 2965–2873 (–CH_2), 1702 [–CO (pos. 2)], 1659 [–CO (pos. 4)], 750 (CH_2).

^{1}H NMR δ = 0.92–0.99 (m, 6H, 2CH_3–CH_2–CH_2), 1.58–1.84 (m, 4H, 2CH_3–CH_2–CH_2), 2.28–2.37 (m, 2H, CH_2–CH_2–CH_2Cl), 3.43–3.63 (m, 2H, CH_2–CH_2–CH_2Cl), 3.92–4.04 (m, 2H, 2CH_3–CH_2–CH_2), 4.49–4.51 (m, 2H, CH_2–CH_2–CH_2Cl).

8.1.2.3. Cyclization. *Method a.* A mixture of 1 mmol of 1,3-dimethyl- or 1,3-dipropyl-7-(3-chloropropyl)-8-bromoxanthine with 4 mol of corresponding benzylamine and 2 ml of DMF was refluxed for 5–10 h. The products were isolated from reaction mixture by adding water and cooling overnight in refrigerator. The crystalline products were filtered off and purified by dissolving in hot ethanol and precipitated with water.

The spectral data are summarized in Table 5.

Method b. A mixture of 0.39 g (1 mmol) of 1,3-dipropyl-7-(3-chloropropyl)-8-bromoxanthine and 4 mmol of benzylamines was melted in microwave oven during 4–10 min (power 300–750 W). After cooling acetonitrile was added and precipitate of the unreacted benzylamine salts was filtered off, the filtrate was evaporated under reduced pressure. To the residue water was added and the precipitated product was collected (compounds **15**, **16**, **18**, **20**). Compound **19** was separated by dissolving the reaction mixture in ethanol and precipitated with water. Compound **17** was isolated from the reaction mixture by adding acetonitrile. The precipitate was washed with water to remove benzylamine salts.

The reaction conditions and the yields are presented in Table 6.

8.2. Adenosine receptor binding assays

Adenosine receptor binding assays were performed as previously described using rat brain cortical membrane preparations for A_1 AR assays and rat brain stratial membrane preparations for A_{2A} assays.[48,53,54] Frozen rat brains (unstripped) were obtained from Pel-Freez®, Rogers, Arkansas, USA. For assays at human A_1, A_{2A}, A_{2B} and A_3 ARs, CHO cell membranes containing the human receptors were used as described.[53,55] [^{3}H]2-chloro-N^6-cyclopentyladenosine ([^{3}H]CCPA) was used as the A_1 radioligand, [^{3}H]3-(3-hydroxypropyllo-7-methyl-8-(*m*-methoxystyryl)-1-propargylxanthine ([^{3}H]-MSX-2) as the A_{2A} radioligand,[56] [^{3}H]4-(2-[7-amino-2-(2-furyl)-[1,2,4]triazolo[2,3-*a*][1,3,5]-triazin-5-4-(amino)-ethyl)phenol ([^{3}H]ZM241385) as the A_{2B} receptor radioligand[57] and [^{3}H]-phenyl-8-ethyl-4-methyl-(8*R*)-4,5,7,8-tetrahydro-1*H*-imidazo-[2,1-*i*]-purine-5-one ([^{3}H]PSB-11) as the A_3 AR radioligand.[22] Initially, a single high concentration of compound (25 μM at A_1 and A_{2A}, 10 μM at A_{2B} and A_3 receptors) was tested in three (A_1, A_{2A}) or two (A_{2B}, A_3) independent experiments. For potent compounds, curves were determined using 6–7 different concentrations of test compounds spanning three orders of magnitude. Data were analyzed using the PRISM program version 3.0 (Graph Pad, San Diego, CA, USA).

8.3. X-ray structure analysis of 8 and 14

Crystal data for **8**: $C_{18}H_{21}N_5O_3$; mol. mass 355.40; triclinic; space group: P-1; $a = 5.0020(10)$ Å; $b = 9.653(2)$ Å; $c = 17.745(4)$ Å; $\alpha = 91.99(3)°$, $\beta = 92.18(3)°$; $\gamma = 91.52(3)°$, $V = 855.3(3)$ Å^3; $z = 2$; d$x = 1.380$ Mg/m^3; $\mu = 0.797$ mm^{-1}; $F(000) = 376$; final $R = 0.064$ for 3549 reflections [$I > 4\sigma(I)$].

Crystal data for **14**: $C_{15}H_{17}N_5O_3$; mol. mass 315.33; monoclinic; space group: $P2_1/n$; $a = 5.1665(8)$ Å; $b = 30.497(4)$ Å; $c = 9.6592(13)$ Å; $\beta = 94.56(1)°$; $V = 1503.0(4)$Å^3; $z = 4$; d$x = 1.394$ Mg/m^3; $\mu = 0.101$ mm^{-1}; $F(000) = 664$; final $R = 0.036$ for 2647 reflections [$I > 4\sigma(I)$].

The crystals of **8** and**14** were obtained by slow evaporation of ethanol solution. The measurement of the crystal **8** was performed on a Kuma4CCD κ-axis diffractometer with graphite-monochromated MoKα radiation at room temperature. The measurement of the crystal **14** was performed on a KM-4 four-cyclic diffractometer with graphite-monochromated CuKα radiation at room temperature. The data were corrected for Lorentz and polarization effects. No absorption correction was applied. All crystallographic data and experimental details are collected in Table 7. The structures were solved by direct methods[58] and refined using SHELXL.[58] The full-matrix least-squares refinement was based on F^2. The positions of all H-atoms were found from electron density $\Delta\rho$ map and refined in raiding model with the isotropic displacement parameters of 1.5 times the respective U_{eq} values for the parent-atoms. Atomic scattering factors were those as in SHELXL.[59] Atomic coordinates are gathered in Table 8. Crystallographic data (excluding structural factors) for the structure reported in this paper have been deposited with the Cambridge Crystallographic Data Center and allocated the deposition numbers: CCDC 623700 for **8** and CCDC 623701 for **14**. Copies of the data can be obtained free of charge on application to CCDC, 12 Union Road, Cambridge CB2 1EW, UK (Fax: Int code + (1223)336-033; E-mail:deposit@ccdc.cam.ac.uk).

8.4. Computational procedures

The starting models of molecules were based on crystallographic data for **8** and **14** using the PCMOD.6 program.[43] The geometry of the molecules was optimised with MOPAC 6.0 using AM1 Hamiltonians in an aqueous environment (dielectric constants equal 78.4).[44]

The values of log*P* and log*D* (at pH 7.4) for the compounds investigated were calculated by means of PALLAS (version 1.2) program.[49] Multiple Linear Regression equations were computed by means of the QSAR-PC:PAR program written by R.C. Coburn.[50]

Acknowledgments

This work was supported by Polish State Committee for Scientific Research (Grant No. 6 P05F 024 21) and by the Deutsche Forschungsgemeinschaft (GRK 677). C.E.M. is grateful for support by the Fonds der Chemischen Industrie and the Bundesministerium für Bildung und Forschung (BMBF), Germany.

Supplementary data

Supplementary data associated with this article can be found, in the online version, at doi:10.1016/j.bmc.2007.04.018.

References and notes

1. Fredholm, B. B.; Arslan, G.; Haldner, L.; Kull, B.; Schulte, G.; Wasserman, W. *Naunyn-Schmiedeberg's Arch. Pharmacol.* **2000**, *362*, 364.
2. Fredholm, B. B.; IJzerman, A. P.; Jacobson, K. A.; Klotz, K.-N.; Linden, J. *Pharm. Rev.* **2001**, *53*, 527.
3. Ralevic, V.; Burnstock, G. *Pharmacol. Rev.* **1998**, *50*, 413.
4. Poulsen, S.-A.; Quinn, R. J. *Bioorg. Med. Chem.* **1998**, *6*, 619.
5. Ferrè, S.; Fredholm, B. B.; Morelli, M.; Popoli, P.; Fuxe, K. *Trends Neurosci.* **1997**, *20*, 482.
6. Ferrè, S.; Popoli, P.; Giménez-Llort, L.; Rimondini, R.; Müller, C. E.; Strömberg, I.; Ögren, S. O.; Fuxe, K. *Parkinsonism Relat. Disord.* **2001**, *7*, 235.
7. Moreau, J.-L.; Huber, G. *Brain Res. Rev.* **1999**, *31*, 65.
8. Müller, C. E. *Drugs Future* **2000**, *25*, 1043.
9. Ongini, E.; Schubert, P. *Drug Dev. Res.* **1998**, *45*, 387.
10. Impagnatiello, F.; Bastia, E.; Ongini, E.; Monopoli, A. *Emerg. Ther. Targets* **2000**, *4*, 635.
11. Ribeiro, J. A.; Sebastião, A. M.; deMendonça, A. *Prog. Neurobiol.* **2003**, *68*, 377.
12. De Sarro, G.; De Sarro, A.; Di Paola, E. D.; Bertorelli, R. *Eur. J. Pharmacol.* **1999**, *371*, 137.

13. Dunwiddie, T. V. *Adv. Neurol.* **1999**, *79*, 1001.
14. McGaraughty, S.; Cowart, M.; Jarvis, M. F.; Berman, R. F. *Curr. Top. Med. Chem.* **2005**, *5*, 43.
15. Hess, S. *Expert. Opin. Ther. Patents* **2001**, *11*, 1.
16. Kieć-Kononowicz, K.; Drabczyńska, A.; Pękala, E.; Michalak, B.; Müller, C. E.; Schumacher, B.; Karolak-Wojciechowska, J.; Duddeck, H.; Rocktt, S.; Wartchow, R. *Pure Appl. Chem.* **2001**, *73*, 1411.
17. Da Settimo, F.; Primofiore, G.; Taliani, S.; Marini, A. M.; La Motta, C.; Novellino, E.; Greco, G.; Lavecchia, A.; Trincavelli, L.; Martini, C. *J. Med. Chem.* **2001**, *44*, 316.
18. Baraldi, P. G.; Tabrizi, M. A.; Bovero, A.; Avitabile, B.; Preti, D.; Fruttarolo, F.; Romagnoli, R.; Varani, K.; Borea, P. A. *Eur. J. Med. Chem.* **2003**, *38*, 367.
19. Ferrarini, P. L.; Betti, L.; Cavallini, T.; Giannaccini, G.; Lucacchini, A.; Manera, C.; Martinelli, A.; Ortore, G.; Saccomanni, G.; Tuccinaroli, T. *J. Med. Chem.* **2004**, *47*, 3019.
20. Yan, L.; Müller, C. E. *J. Med. Chem.* **2004**, *47*, 1031.
21. Müller, C. E. *Curr. Top. Med. Chem.* **2003**, *3*, 445.
22. Müller, C. E.; Diekmann, M.; Thorand, M.; Ozola, V. *Bioorg. Med. Chem. Lett.* **2002**, *12*, 501.
23. Shimada, J.; Suzuki, F.; Nokada, H.; Ishii, S.; Ichikawa, S. *J. Med. Chem.* **1992**, *36*, 2342.
24. Nonaka, H.; Ichimura, M.; Takeda, M.; Nonaka, Y.; Shimada, J.; Suzuki, F.; Yamaguchi, K.; Kase, H. *Eur. J. Pharmacol., Mol. Pharm. Sect.* **1994**, *267*, 335.
25. Jacobson, K. A.; Gallo-Rodriguez, C.; Melman, N.; Fischer, B.; Maillard, M.; van Bergen, A.; van Galen, P. J. M.; Karton, Y. J. *J. Med. Chem.* **1993**, *36*, 1333–1342.
26. Jackson, E. K.; Herzer, W. A.; Suzuki, F. *J. Pharmacol. Exp. Ther.* **1993**, *267*, 1304.
27. Nonaka, Y.; Shimada, J.; Nonaka, H.; Koike, N.; Aoki, N.; Kobayashi, H.; Kase, H.; Yamaguchi, K.; Suzuki, F. *J. Med. Chem.* **1993**, *36*, 3731.
28. Hockemeyer, J.; Burbiel, J. C.; Müller, C. E. *J. Org. Chem.* **2004**, *69*, 3308.
29. Müller, C. E.; Sandoval-Ramirez, J.; Schobert, U.; Geis, U.; Frobenius, W.; Klotz, K. N. *Bioorg. Med. Chem.* **1998**, *6*, 707.
30. Sauer, R.; Maurinsh, J.; Reith, U.; Fülle, F.; Klotz, K. N.; Müller, C. E. *J. Med. Chem.* **2000**, *43*, 440.
31. Knutsen, L. J. S.; Weiss, S. M. *Curr. Opin. Invest. Drugs* **2001**, *2*, 668.
32. Rabasseda, X.; Sorbera, L. A.; Martin, L.; Leeson, P. A.; Castañer, J. *Drugs Future* **2001**, *26*, 20.
33. Drabczyńska, A.; Müller, C. E.; Lacher, S. K.; Schumacher, B.; Karolak-Wojciechowska, J.; Nasal, A.; Kawczak, P.; Yuzlenko, O.; Pękala, E.; Kieć-Kononowicz, K. *Bioorg. Med. Chem.* **2006**, *14*, 7258.
34. Sauer, R.; Maurinsh, J.; Reith, U.; Fülle, F.; Klotz, K.-N.; Müller, C. E. *J. Med. Chem.* **2000**, *43*, 440.
35. Drabczyńska, A.; Schumacher, B.; Müller, C. E.; Karolak-Wojciechowska, J.; Michalak, B.; Pękala, E.; Kieć-Kononowicz, K. *Eur. J. Med. Chem.* **2003**, *38*, 397.
36. Drabczyńska, A.; Müller, C. E.; Schumacher, B.; Hinz, S.; Karolak-Wojciechowska, J.; Michalak, B.; Pękala, E.; Kieć-Kononowicz, K. *Bioorg. Med. Chem.* **2004**, *12*, 4895.
37. Rockitt, S.; Wartchow, R.; Duddeck, H.; Drabczyńska, A.; Kieć-Kononowicz, K. *Z. Naturforsch.* **2001**, *56B*, 319.
38. Eckstein, M.; Łosoń, W. *Dissert. Pharm. Pharmaceut.* **1968**, *20*, 35.
39. Papesh, V.; Grove, M.; Schroeder, E. F.; Serle, G. D. United States Patent 1952, 2, 602.795; *Chem. Abstr.* **1953**, *47*, 4920f.
40. Kramer, G. L.; Garst, J. E.; Mitchel, S. S.; Wells, J. N. *Biochemistry* **1997**, *16*, 3316–3321.
41. Bergmann, F.; Dickstein, S. *J. Am. Chem. Soc.* **1955**, *77*, 691.
42. Rybar, A.; Antoš, K. *Coll. Czech. Chem. Commun.* **1970**, *35*, 1415.
43. PCMODEL 6 Molecular Modeling Software for the IBM PC, Serena Software, Bloomington, 1996.
44. MOPAC program version 6, QCPE No. 455; Department of Chemistry, Indiana University, Bloomington, IN 47405, 1990.
45. Müller, C. E.; Maurinsh, J.; Sauer, R. *Eur. J. Pharm. Sci.* **2000**, *10*, 259.
46. Klotz, K.-N.; Lohse, M. J.; Schwalbe, U.; Cristalli, G.; Vittori, S.; Grifantini, M. *Naunyn-Schmiedeberg's Arch. Pharmacol.* **1989**, *340*, 679.
47. Gao, Z. G.; IJzerman, A. P. *Biochem. Pharmacol.* **2000**, *60*, 669.
48. Hayallach, A. M.; Sandoval-Ramirez, J.; Reith, U.; Preiss, B.; Schumacher, B.; Daly, J. W.; Müller, C. E. *J. Med. Chem.* **2002**, *45*, 1500.
49. PALLAS for Windows 1.2, CompuDrug Chemistry LTD, 1995.
50. QSAR-PC program, R. A. Coburn; BIOSOFT, Cambridge, UK.
51. Da Settimo, F.; Primofiore, G.; Taliani, S.; Marini, A. M.; La Motta, C.; Novellino, E.; Greco, G.; Lavecchia, A.; Trincavelli, L.; Martini, C. *J. Med. Chem.* **2001**, *44*, 316.
52. Bondavalli, F.; Botta, M.; Bruno, O.; Ciacci, A.; Corelli, F.; Fossa, P.; Lucacchini, A.; Manetii, F.; Martini, C.; Menozzi, G.; Mosti, L.; Ranise, A.; Schenone, S.; Tafi, A.; Trincavelli, M. A. *J. Med. Chem.* **2002**, *45*, 4875.
53. Müller, C. E.; Thorand, M.; Quirshi, R.; Dieckmann, M.; Jacobson, K. A.; Padgett, W. L.; Daly, J. W. *J. Med. Chem.* **2002**, *45*, 3440–3450.
54. Hess, S.; Müller, C. E.; Frobenius, W.; Reith, U.; Klotz, K.-N.; Eger, K. *J. Med. Chem.* **2000**, *43*, 4636–4646.
55. Klotz, K.-N.; Hessling, J.; Hegler, J.; Owman, C.; Kull, B.; Fedholm, B. B.; Lohse, M. J. *Naunyn-Schmiedeberg's Arch. Pharmacol.* **1998**, *357*, 1–9.
56. Müller, C. E.; Maurinsh, J.; Sauer, R. *Eur. J. Pharm. Sci.* **2000**, *10*, 259–265.
57. Ji, X.-D.; Jacobson, K. A. Use of the triazolotriazine [^{3}H]ZM 241385 as a radioligand at recombinant human A_{2B} adenosine receptors. *Drug Des. Discov.* **1999**, *16*, 217–226.
58. Sheldrick, G. M. *SHELXL-93. A FORTRAN-77 Program for the Refinement of Crystal Structures from Diffraction Data*; University of Göttingen: Germany, 1993.
59. Sheldrick, G. M. *SHELXTL PC*^{MT}; Siemens Analytical X-Ray Instruments Inc.: Madison, Wisconsin, USA, 1990.